PROCEEDINGS OF SCIENCE

Estimation of Temporal and Spatial Distributions of High-Energy Cosmic-Ray Electron Sources using Genetic Algorithms

Shunji Igarashi[a] **and Kenji Yoshida**[a,*]

[a] *Shibaura Institute of Technology*
307 Fukasaku, Minuma-ku, Saitama 337-8570, JAPAN

E-mail: bp19115@shibaura-it.ac.jp, yoshida@shibaura-it.ac.jp

Over the last decade, precise high-energy cosmic-ray electron + positron energy spectra have been obtained with superior instruments such as CALET. Their energy spectra, which exhibit characteristic structures, have the potential to reveal the origin of cosmic-ray electrons. Although supernova remnants (SNRs) are the most likely candidates for high-energy cosmic-ray electrons, the locations of the acceleration sources of observed cosmic-ray electrons, as well as the epoch of their emission from these sources, remain undetermined. In this work, we estimate the temporal and spatial distributions of SNRs in the Galaxy from the observed CALET electron + positron spectrum. We apply genetic algorithms to represent the observed electron + positron spectrum with the calculated flux of high-energy electrons from SNRs distributed in the Galaxy. We identified the clustering features of the estimated SNR distribution as a function of age and distance, not only including the ages and distances of the known nearby SNRs but also extending beyond these known SNRs. Our results are consistent with the SNR origin hypothesis of high-energy cosmic ray electrons, and they also predict that several unknown SNRs are likely to be located in the clustering regions.

39th International Cosmic Ray Conference (ICRC2025)
15–24 July 2025
Geneva, Switzerland

ICRC 2025
The Astroparticle Physics Conference
Geneva July 15-24, 2025

*Speaker

PoS(ICRC2025)159

1. Introduction

As light leptons, high-energy cosmic-ray electrons (positrons) rapidly lose energy proportional to the square of their energy during propagation in the Galaxy. Since TeV electrons lose most of their energy on a timescale of 10^5 yr, and their propagation distances are therefore limited to several hundred parsecs, only a limited number of cosmic-ray electron sources can contribute to TeV-region electrons, resulting in discrete source effects such as structure in the electron + positron spectrum and the anisotropy favoring the source direction. Consequently, observations of TeV electrons are anticipated to enable the identification of cosmic-ray electron acceleration sources [1].

The presence of electrons and/or positrons in cosmic rays can be attributed to some potential origins. The primary candidates for cosmic-ray negative electrons are supernova remnants (SNRs), which are the primary accelerators of cosmic-ray electrons themselves. The second is the secondary production of electrons and positrons as byproducts of interactions between primary cosmic rays (mostly protons and heavier nuclei) and the interstellar medium. The positron observations by PAMELA and AMS-02 have revealed that the fraction of positrons increases with energy above ~10 GeV, contrary to expectations from purely secondary production [2, 3]. The third is the anomalous positron abundance that has led to speculation about other potential primary sources of electrons and positrons, such as dark matter and pulsars. Nevertheless, the locations of the acceleration sources of observed high-energy cosmic-ray electrons, as well as the epoch of their emission from these sources, remain undetermined.

Over the last decade, precise high-energy cosmic-ray electron + positron energy spectra have been obtained with superior instruments such as DAMPE, Fermi-LAT, AMS-02, CALET, and H.E.S.S. [4–8]. Their energy spectra, which exhibit characteristic structures, have the potential to reveal the origin of cosmic-ray electrons, with supernova remnants (SNRs) being the most likely candidates. This work aims to determine the spatial and emission time distribution of high-energy cosmic ray electron sources in the Galaxy, focusing on the cosmic-ray electron + positron energy spectrum observed with CALET. This work enables us to verify the SNR origin hypothesis of cosmic-ray electrons and to predict the ages and distances of unknown SNRs.

2. Methods

2.1 Modeling of cosmic-ray electron + positron spectra

By calculating the superposition of electron + positron spectra from individual sources and reproducing the observed cosmic-ray electron + positron spectra, we estimate the locations of the acceleration sources for high-energy cosmic-ray electrons within the Galaxy and the time elapsed since their emission.

The cosmic-ray electron spectrum $J(E, r, t)$ with the electron energy E from an SNR with an injection spectrum $Q(E) = Q_0 E^{-\gamma} \exp(-E/E_c)$ at a distance r and time t after the release of electrons from an SNR is derived from the diffusion equation, described in Kobayashi *et al.* (2004) [1]. Here, Q_0 is a normalization factor, γ is a power-law index, and E_c is an exponential cutoff energy. Taking the electron energy-loss rate given by $dE/dt = -bE^2$ and the diffusion

coefficient with the form $D = D_0 E^{\delta}$, the $J(E, r, t)$ is given by

$$J(E, r, t) = \frac{c}{4\pi} \frac{1}{(4\pi D_1)^{3/2}} e^{-r^2/(4D_1)} Q(\frac{E}{1-bEt})(1-bEt)^{-2} e^{-E/(E_c(1-bEt))}, \quad (1)$$

where c is the speed of light and

$$D_1 = \int_E^{E/(1-bEt)} (1/b) D E^{-2} dE.$$

The positron spectral formula from Eq. (4) of M. Aguilar *et al.* (2019) [3] provides the secondary positron spectrum, as well as the anomalous positron component such as dark matter and pulsars. We use the twofold positron spectral formula to describe both electrons and positrons of the secondary and anomalous positron components.

We determined the source and propagation parameters by fitting the observed CALET electron + positron spectrum using analytical formulas for continuously and uniformly distributed SNRs, taking the secondary and anomalous positron sources into account. The SNR component has a summation formula of Eq.(1), described in Eq.(A3) of Kobayashi et al. (2004) [1]. As described in Kobayashi et al. (2004) [1] and shown in the previous studies of Monte-Carlo (M.C.) simulation energy spectra (e.g. [9]), as well as presented in Fig. 1, the diversity of the spatial and age distributions causes the spectral shape variation that is larger with the higher energies. To avoid variations in the spectral shape at higher energies, we used a lower energy range of $10-200$ GeV for spectral fitting to determine the source and propagation parameters. As a result, the output electron energy from an SNR above 1 GeV is $W = 9.68\times10^{47}$ erg, taking the supernova rate of 1/40 yr in the Galaxy. The power-law index of the injection spectrum is $\gamma = 2.54$, taking the cutoff energy $E_c = 20$ TeV. The diffusion coefficient spectral index is fixed to be $\delta = 0.52$ referring to the B/C ratio observed with CALET in the energy range of 25—3800 GeV/n [10], taking $D_0 = 2.0\times10^{28}$ (cm^2 s^{-1}). The source and propagation parameters are summarized in Table 1.

Table 1: Summary of source and propagation parameters

W (erg)	γ	E_c	D_0 (cm^2 s^{-1})	δ	SN rate
9.68×10^{47}	2.54	20 TeV	2.0×10^{28}	0.52	1/40 yr

2.2 Genetic Algorithms

Genetic Algorithms (GAs) are a class of metaheuristic optimization algorithms inspired by the process of natural selection and evolution in biology (e.g., [11]). GAs operate on a population of candidate solutions, where better-optimized individuals have a higher probability of passing their characteristics to the next generation. The iterative process leads to the gradual improvement of the individuals over generations, ultimately converging toward an optimal or near-optimal solution. In this work, a candidate solution represented as an individual is encoded as a list of genes, which are pairs of the distance (r) to and age (t) of an SNR, as follows:

$$(r_1, t_1), (r_2, t_2), \cdots, (r_{n-1}, t_{n-1}), (r_n, t_n).$$

Whose length (i.e., the number of genes) corresponds to the number of SNRs of the individual. These individuals provide the calculated electron energy spectra based on Eq.(1) in section 2.1. A group of these individuals forms the population. The fitness function, which evaluates the quality of each individual, is the χ^2 value between the observed and calculated electron energy spectra. The GA procedure in this work is outlined below.

1. A population consisting of 40 individuals is initialized randomly.
2. The fitnesses of each individual of the population are calculated.
3. Roulette selection and Crossover operators: Some (35 %) individuals are probabilistically selected from the current population to act as parents for the next generation, with better-fitted individuals having a higher chance of selection, namely roulette selection. The selected individuals exchange genetic material using a single-point crossover operator, producing the same number of new offspring as they have.
4. Mutation operator: A uniform mutation operator is applied to some (15 %) current individuals at a random gene to produce offspring, ensuring diversity within the population and preventing premature convergence to local optima.
5. Elite selection operator: Some (50 %) of the best-fitted individuals from the current population are directly copied into the next generation as elite selection without undergoing crossover or mutation.
6. The new offspring population replaces the current population, forming the next generation. This iterative process continues until a maximum of $N = 1200$ generations.

The GA parameters are summarized in Table 2.

Table 2: Summary of GA parameters

Individuals	Elite	Crossover	Mutation	Fitness	Generations
40	50 %	35 %	15 %	χ^2	1200

2.3 Application of GA to cosmic-ray electron + positron spectra

SNRs are generated at random in the Galactic disk of a radius of 10 kpc with a supernova rate of $1/40$ yr at the maximum age of 1×10^8 yr. The Solar system is located at a distance of 8.5 kpc from the Galactic center. An electron energy spectrum of an SNR is calculated with Eq.(1). Figure 1 presents the M.C. simulation energy spectrum of the total SNRs (2.5×10^6) for 200 trials with the solid red line, including the secondary production and the positron anomalous component, illustrating the 1 σ spectral variation with the red region. We need the enormous computational cost to apply the GA with the total number of SNRs of 2.5×10^6. To avoid the enormous computational cost of the GA, we separate the distant SNRs from the nearby SNRs in time and space. The distant and nearby SNR components are the electron energy spectra of the distant SNRs, except within

thresholds of age and distance, and of the nearby SNRs, within the thresholds of age and distance. We set the thresholds of ages and distances to be 90 kyr and 0.70 kpc, respectively. Figure 1 also presents the M.C. simulation energy spectrum of the distant SNR component, including the secondary production and the anomalous positron source, with the dashed green line, illustrating the 1 σ spectral variation with the green region. As shown in Fig. 1, the distant component spectrum has less spectral variation than that of the total component spectrum. The 1 σ spectral variations of the distant component spectrum are less than about half of the uncertainties of the electron + positron fluxes observed with CALET in the energy range of 10 GeV − 7.5 TeV. The GA is applied to generate the nearby 11 SNRs in time and space with the source and propagation parameters described in Table 1. The distant SNR component is characterised by the typical distant SNR spectrum, as well as the secondary and anomalous positron components, which have the fixed electron + positron energy spectra. The generated electron + positron spectrum, comprising the nearby SNR, distant SNR, secondary, and anomalous positron components, is optimized to represent the CALET cosmic-ray electron + positron spectrum by using the GA. We applied 1000 trials of the GA optimization.

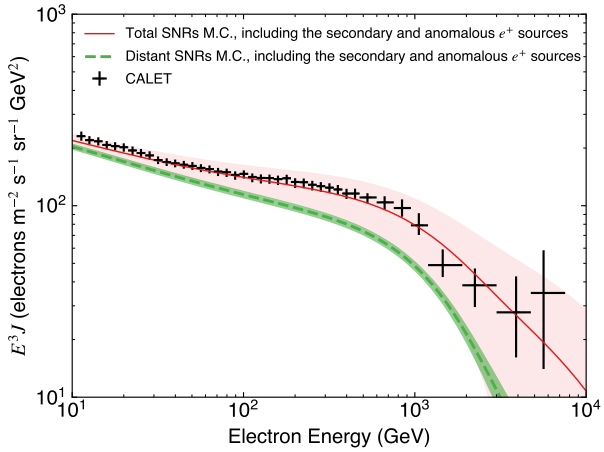

Figure 1: The M.C. simulation energy spectra of total and distant SNRs, including the secondary electrons and positrons, and the anomalous positron component that includes electrons. The solid red and dashed green lines represent the average spectra of the total and distant SNRs, respectively, illustrating the 1σ spectral variation with red and green regions. The crosses represent the cosmic-ray electron + positron spectrum observed with CALET [7].

3. Results

Figure 2 shows a typical example of the age-distance scatter plot of the optimized 11 SNRs by using the GA (upper left panel) and their electron energy spectra with solid lines. The 3 SNRs with ages less than 40 kyr and distances of 0.2 – 0.5 kpc contribute 10^2 – 10^4 GeV electrons (lower left panel). The 5 SNRs with ages above 40 kyr and distances of 0.4 – 0.6 kpc contribute 10^2 – 10^3 GeV electrons (upper right panel). The 3 SNRs with ages above 40 kyr and distances less than 0.1 kpc contribute 10^1 – 10^3 GeV electrons (lower right panel).

Figure 3 presents the χ^2 distribution of 1000 trials with the GA. The mean and standard deviation of χ^2 are 6.79 and 0.51 for the degree of freedom (d.o.f.) of 17. Figure 4 presents the typical energy spectrum of electrons + positrons with the GA for χ^2 = 6.79. Figure 5 illustrates the estimated SNR distribution as a function of age and distance, filtered with $E^3J >$ 0.5 m^{-2}s^{-1}sr^{-1}GeV^2 at 1 TeV to focus on around the TeV region. The color bar indicates the

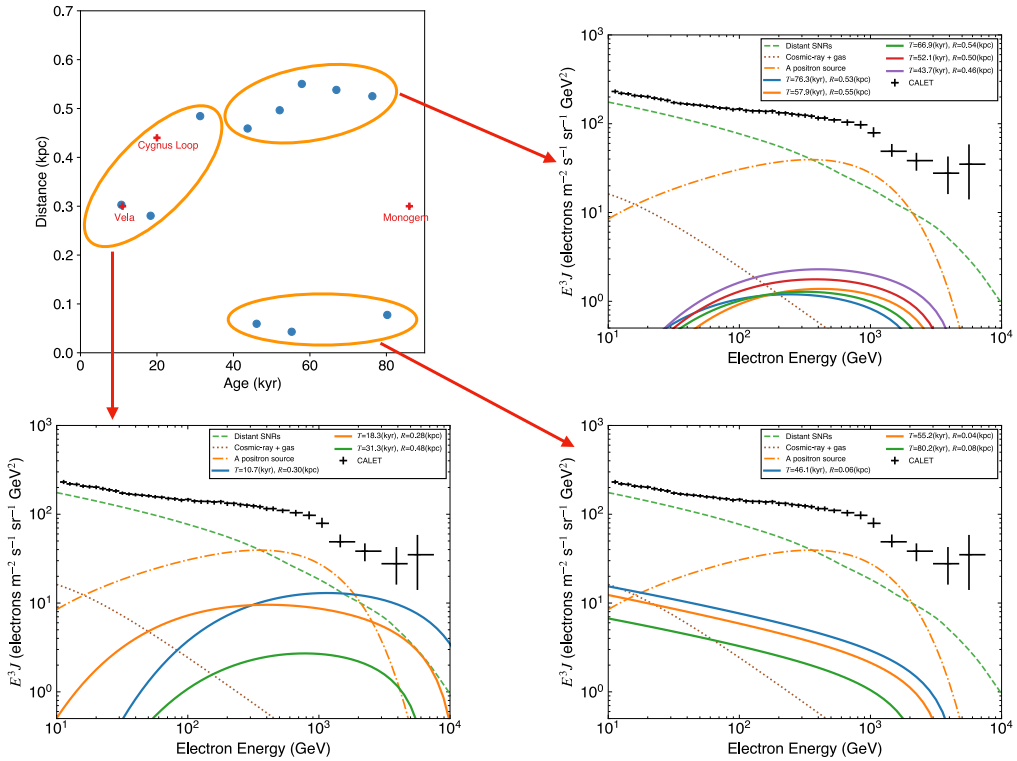

Figure 2: An age-distance scatter plot of a typical individual with 11 nearby SNRs (upper left panel) and their electron energy spectra with solid lines (upper right and lower panels). The locations of the nearby SNRs Vela, Cygnus Loop, and Monogem are marked with red crosses in the upper left panel. The energy spectra of the distant SNR, secondary, and anomalous positron components are presented in the short-dashed green line, dotted brown line, and dot-dashed orange line, respectively. The black crosses represent the CALET electron + positron energy spectrum.

expected number of SNRs per bin. The locations of the nearby SNRs Vela, Cygnus Loop, and Monogem are marked with red crosses. The clustering features appear in Fig. 5, not only including the ages and distances of the known nearby SNRs, but also extending beyond the known SNRs.

4. Discussion and Conclusions

We applied GA to estimate the age-distance distributions of nearby SNRs from the CALET electron + positron energy spectrum. As shown in Fig. 3, the fitnesses of χ^2 with d.o.f = 17 for 1000 trials suggest the validity of the optimization with the GA. As presented in Fig. 5, we found the clustering features of the estimated SNR distribution as a function of age and distance. While the expected number of nearby SNRs within the age of 90 kyr and the distance of 0.70 kpc is about 11, the known nearby SNRs of Vela and Cygnus Loop are located in the middle left clustering in Fig. 5, and the known SNR Monogem is in the tail of the lower clustering in Fig. 5. These results are consistent with the SNR origin hypothesis of high-energy cosmic ray electrons, as well as predict that around eight unknown SNRs are likely to be located in the clustering regions in Fig. 5.

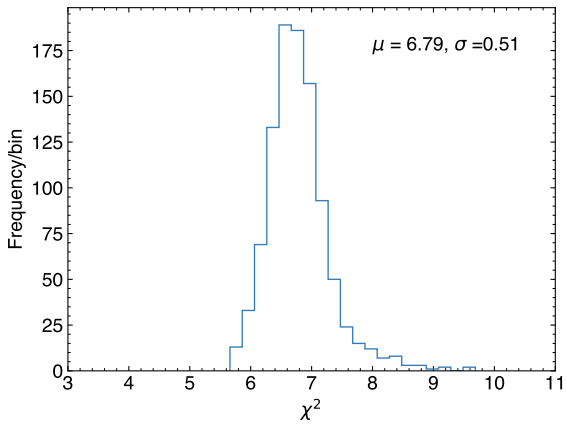

Figure 3: The χ^2 distribution of 1000 trials with the GA. The mean and standard deviation of χ^2 is 6.79 and 0.51.

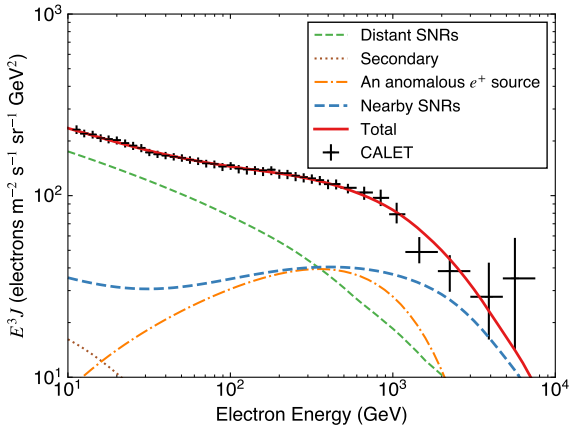

Figure 4: The typical energy spectrum with the GA for $\chi^2 = 6.79$. The solid red and dashed blue lines represent the total and nearby SNR energy spectrum, compared with the CALET electron + positron energy spectrum. The other lines and symbols of the energy spectra are the same as Fig. 2.

References

[1] T.Kobayashi, Y. Komori, K.Yoshida & J.Nishimura, *The Most Likely Sources of High-Energy Cosmic-Ray Electrons in Supernova Remnants*, *ApJ* **601** (2004) 340 [astro-ph/0308470]

[2] O.Adriani, G.C.Barbarino, G.A.Bazilevskaya, *et al.*, *An anomalous positron abundance in cosmic rays with energies 1.5-100GeV*, *Nautre* **458** (2009) 607 [astro-ph/0810.4995]

[3] M.Aguilar, L. Ali Cavasonza, G.Ambrosi, *et al.*, *Towards Understanding the Origin of Cosmic-Ray Positrons*, *Phys. Rev. Lett.* **122** (2019) 041102

[4] J.Chang, J.H. Adams, H.S.Ahn, *et al.*, *An excess of cosmic ray electrons at energies of 300-800GeV*, *Nature* **456** (2008) 362

[5] S.Abdollahi, M.Ackermann, M. Ajello, *et al.*, *Cosmic-ray electron-positron spectrum from 7 GeV to 2 TeV with the Fermi Large Area Telescope*, *Phys. ReV. D* **082007** (2017) 082007 [astro-ph.HE/1704.07195]

[6] M.Aguilar, L. Ali Cavasonza, B.Alpat, *et al.*, *Towards Understanding the Origin of Cosmic-Ray Electrons*, *Phys. Rev. Lett.* **122** (2019) 101101

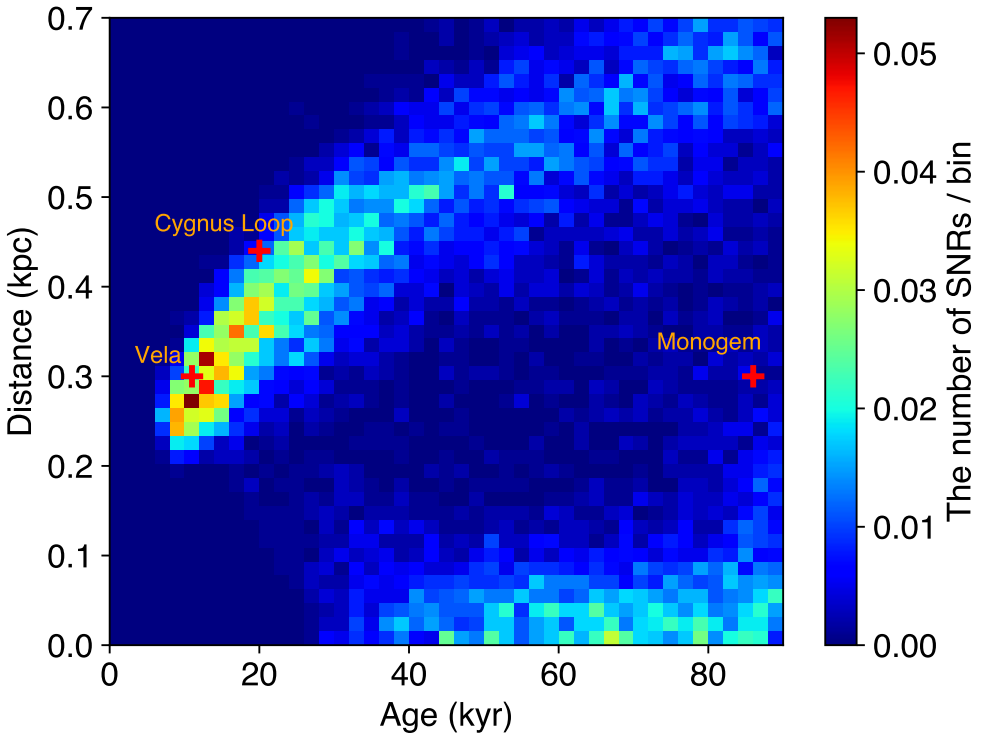

Figure 5: The estimated nearby SNR distribution as a function of age and distance, filtered with $E^3J > 0.5\ \mathrm{m^{-2}s^{-1}sr^{-1}GeV^2}$ at 1 TeV. The color bar corresponds to the expected number of SNRs per bin. The red crosses are the same as Fig. 2.

[7] O.Adriani, Y.Akaike, K.Asano, *et al.*, *Direct Measurement of the Spectral Structure of Cosmic-Ray Electrons+Positrons in the TeV Region with CALET on the International Space Station*, *Phys. Rev. Lett.* **131** (2023) 191001 [astro-ph.HE/2311.05916]

[8] F.Aharonian, F.Ait Benkhali, J.Aschersleben, *et al.*, *High-Statistics Measurement of the Cosmic-Ray Electron Spectrum with H.E.S.S.*, *Phys. Rev. Lett.* **133** (2024) 221001 [astro-ph.HE/2411.08189]

[9] K.Asano, Y.Asaoka, Y.Akaike, *et al.*, *Monte Carlo Study of Electron and Positron Cosmic-Ray Propagation with the CALET Spectrum*, *Astrophys. J.* **926** (2022) 5 [astro-ph.HE/2111.09636]

[10] O.Adriani, Y.Akaike, K.Asano, *et al.*, *Cosmic-Ray Boron Flux Measured from 8.4 GeV /n to 3.8 TeV /n with the Calorimetric Electron Telescope on the International Space Station*, *Phys. Rev. Lett.* **129** (2022) 251103 [astro-ph.HE/2212.07873]

[11] S.Katoch, S.S.Chauhan & V.Kumar, *A review on genetic algorithm: past, present, and future*, *Multimedia Tools and Applications* **80** (2021) 8091